JOURNAL OF CATALYSIS 91, 1–10 (1985)

Disproportionation of CO on Small Particles of Silica-Supported Palladium

S. ICHIKAWA, H. POPPA, AND M. BOUDART[1]

Stanford/NASA–Ames Joint Institute of Surface and Microstructure Research, Department of Chemical Engineering, Stanford University, Stanford, California 94305

Received March 1, 1984; revised July 30, 1984

Adsorption and desorption cycles of CO were investigated on silica-supported palladium with different values of D, the percentage of metal exposed. With high values of D (100 and 75.4%), carbon accumulated on the metal as a result of the cycling. Further results showed that disproportionation of CO to CO_2 and carbon on palladium occurs on small particles, but not on larger ones. This finding suggested that the selectivity of CO–H_2 reactions might shift to methane at the expense of methanol with decreasing palladium particle size. This shift in selectivity was observed at 535 kPa. At atmospheric pressure, the turnover rate for methane production increases as palladium particle size decreases. Thus methanation on palladium is structure-sensitive, like the disproportionation of CO.

INTRODUCTION

Adsorption of CO on transition metals has been investigated extensively. Numerous data have been accumulated since the review by Ford (*1*). A key question is whether the diatomic molecule in its interaction with metal surfaces remains molecular or dissociates into carbon and oxygen atoms or undergoes disproportionation. This question is crucial in the elucidation of the mechanism of reactions between CO and H_2 on group VIII metals (*2*).

Brodén *et al.* (*3*) have estimated the perturbation of molecular orbitals for CO adsorbed on transition metals at room temperature (RT). Of the nine metals in group VIII, it was predicted that only iron could dissociate CO. However, in recent years, dissociation of CO at relatively mild temperatures on other metals in group VIII has been observed. It occurs at 400 K on nickel (*4*). Bond scission of CO is less expected on more noble metals. Yet there is evidence of carbon deposition following adsorption of CO on ruthenium at 415 K (*5*) and rhodium at 473 K (*6*). As for palladium, Doering *et al.* (*7, 8*) gave indications of carbon deposition below 550 K on the metal particles but only when they are sufficiently small (below about 5 nm).

Recently, many studies have focused on the reaction between CO and H_2 on group VIII metals. On nickel [evaporated film (*9*), Ni/SiO_2 (*10, 11*)] methanation occurs via hydrogenation of surface carbon deposited by CO. Such a reaction route was also favored for ruthenium [evaporated film (*12*), Ru/SiO_2 (*10, 11*)] and on rhodium [Rh/SiO_2, Rh/Al_2O_3 (*13*)]. In the case of palladium, a variety of interesting results were obtained. Vannice found the turnover rate on Pd/η-Al_2O_3 to be more than an order of magnitude higher than that on Pd/SiO_2 for methanation at atmospheric pressure, and the selectivity was 100% to methane in both cases (*14*). Poutsma *et al.* observed high selectivity to methanol on both Pd/SiO_2 and Pd/γ-Al_2O_3 at above ~1 MPa, and the rate of methanol formation did not change appreciably with nature of the support (*15*). Activity and selectivity were shown to vary when palladium was with different kinds of silica (*16*) as well as with several unconven-

[1] To whom correspondence should be addressed.

0021-9517/85 $3.00

tional metal oxide supports (*17*). Certain alkali additives have an effect on $CO-H_2$ reactions on Pd/SiO_2. Whereas sodium did not affect methanation rate (*18*), lithium and sodium increased the selectivity toward methanol formation (*19*). Poels *et al.* (*20*) suggested that palladium atoms with oxidation state higher than zero are the essential sites for methanol formation.

The present work shows the results of interaction between CO and small palladium particles. The results of dependence of particle size on the selectivity of the reaction between CO and H_2 on palladium are also reported.

EXPERIMENTAL

The samples were prepared by cation exchange between silica and a $[Pd(NH_3)_4]Cl_2$ solution (*21*). In order to remove contaminants the support (Davison silica gel, grade 62, 60/200 mesh) was acid-washed (*22*). The unwashed support contained 99 ppm iron, 8 ppm cobalt, 6 ppm nickel, 368 ppm sodium, and an undetectable amount of lithium (below 0.1 ppm). The acid treatment gave samples with undetectable amounts of all these metals except for 35 ppm sodium. The exchanged support was outgassed (10^{-4} Pa) at room temperature (RT), then $Pd(NH_3)_4^{2+}$ ions were decomposed in flowing dioxygen as the temperature was raised slowly to 723 K and held there for 4 h. The first sample, 1.36% Pd/SiO_2, was outgassed at 673 K and reduced at this temperature in flowing dihydrogen while increasing its pressure slowly to atmospheric pressure and held there for 2 h. The other two samples, 1.88% Pd/SiO_2-A and 1.88% Pd/SiO_2-B, were prepared in the same batch, and they were treated in accordance with the above procedure except for reduction temperatures of 723 and 973 K, respectively. The palladium loading is expressed in weight percentage (1.36 and 1.88 wt%), and it was determined by atomic absorption.

As to the gases used in this work, dihydrogen was passed through a palladium thimble (Model CH-A Milton Roy Co.) or through an Engelhard Deoxo unit followed by a molecular sieve trap at 78 K. Carbon monoxide (Matheson research grade 99.99% min.) and also helium (Matheson 99.995% min.) used for dead-volume measurements were passed through molecular sieve traps at 195 and 78 K, respectively.

Values of D, the percentage of metal exposed, were determined by dihydrogen chemisorption at RT. A sample was evacuated (10^{-4} Pa) at 673 K and reduced at this temperature for 1 h in flowing dihydrogen followed by 2-h evacuation at 673 K. Then adsorption isotherms were obtained. More detailed procedure is described elsewhere (*21*). The amount of chemisorbed CO was determined by the same method as above.

High-resolution bright field electron micrographs of the samples before and after adsorption and desorption experiments were obtained with a Hitachi 500-H machine at 100 kV. Samples were deposited on perforated carbon films supported on copper grids. The average particle diameter and the particle size distribution for each sample were obtained by taking micrographs from different areas which totaled to about 2500 particles and by measuring them with a particle size analyzer (Carl Zeiss TGZ3). Through-focus micrographs were taken to find the optimum defocus conditions. In all cases, direct magnification was 2.4×10^5 and photographic enlargement was up to 6.24×10^5.

Adsorption and desorption of CO were followed by a FT-ir spectrometer (NICOLET Model 7199). All spectra were obtained between 400 and 4000 cm^{-1} resolution by means of a HgCdTe detector cooled by liquid N_2. Background spectra were taken after reduction and evacuation of the samples prior to introducing CO. Finely ground powder (8 mg) was pressed into a disk 1.25 cm in diameter.

The reaction of $CO-H_2$ mixtures was studied in flow systems. A conventional Pyrex glass apparatus was used for operations between atmospheric pressure and 202 kPa, and stainless-steel tubings were used at 535

TABLE 1

Determination of Metal Particle Size by Dihydrogen Chemisorption and BFEM[a]

Sample of Pd/SiO_2 (wt% Pd)	Percentage of metal exposed D (%)	Particle size (nm)	
		From D[b]	From BFEM
1.36	100	1.1	<1.0
1.88-A	75.4	1.5	1.4
1.88-B	45.4	2.5	2.4

[a] Bright-field electron microscopy.

[b] Sphere of average diameter, d_{av}, was assumed; $d_{av} = [6(V_{Pd}/A_{Pd})/D] = 1.12/D$ where V_{Pd} is the atomic volume at 293 K equal to 1.47×10^{-2} nm³/Pd atom and A_{Pd} is the atomic area of palladium equal to 7.895×10^{-2} nm²/Pd atom obtained by taking arithmetic average of the number densities of low index planes, viz. {111}, {100}, {110}.

kPa with a precision variable leak valve (Series 293 Granville-Phillips Co.) connected to a gas chromatograph (Aerograph Model A-90-P3) equipped with Porapak Q column used at different temperatures.

RESULTS AND DISCUSSIONS

Adsorption of CO

In Table 1, the results for the characterization of freshly prepared samples by chemisorption are compared with those obtained by electron microscopy. Good agreement can be seen between the two methods. Carbon monoxide adsorption and desorption cycles were performed on these samples in a static closed system. Carbon monoxide was adsorbed at RT and at 50 kPa followed by evacuation to 10^{-4} Pa leaving only chemisorbed CO. Then the sample system was closed and isolated from the pumping system. The desorbed amount of gas at 673 K (A_{des}) and readsorbed amount of gas at 298 K (A_{read}: data at RT were corrected to 298 K) were measured and normalized by the first A_{des} value. Also for comparison, these values were corrected so that they were based on the same total surface area obtained in Table 1 for all samples. The results are shown in Fig. 1. For 1.36% Pd/SiO_2 and 1.88% Pd/SiO_2-A, the pressures at 673 K decreased, whereas the pressures at 298 K increased as the cycle was repeated. That is, there were large decreases in A_{des} and also in A_{read} until the changes became small after four cycles. These trends were more significant with the smaller palladium particles. On the other hand, these changes were negligibly small in the case of 1.88% Pd/SiO_2-B. If palladium particles remained stable and not sintered under CO between RT and 673 K and if CO adsorbs and desorbs as molecules, both A_{des} and A_{read} should stay constant. The decrease in A_{des} indicated a possibility of CO disproportionation. Then the total number of species in the gas phase decreases and thus the pressure drop at 673 K at each cycle. The decline in A_{read} suggested blocking of CO adsorption sites by the deposited carbon until all of the responsible sites were covered by the carbon. It is the above simple experiment which prompted us to investigate the interaction of CO with small palladium particles.

Characterization of the samples before and after seven heating cycles by CO

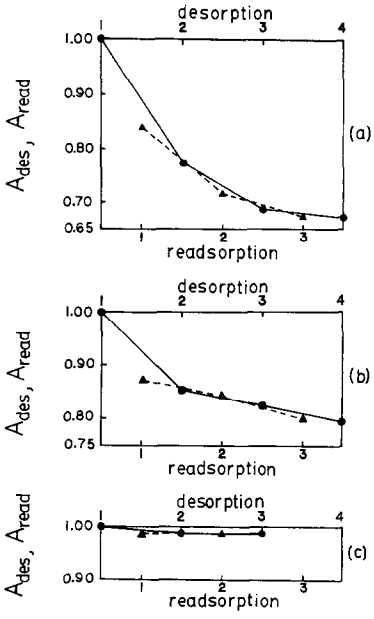

FIG. 1. Changes in desorbed and readsorbed amounts. A_{des} (●) = desorbed amount at 673 K. A_{read} (▲) = readsorbed amount at 298 K. (a) 1.36% Pd/SiO_2, (b) 1.88% Pd/SiO_2-A, (c) 1.88% Pd/SiO_2-B.

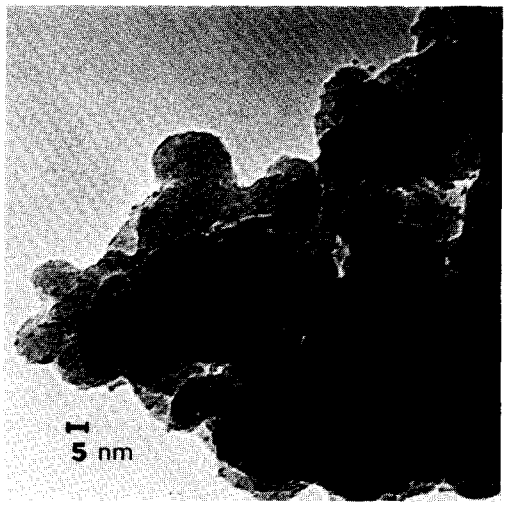

a BEFORE

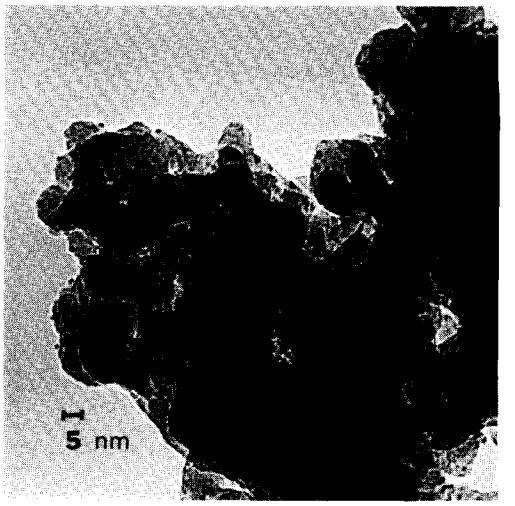

AFTER

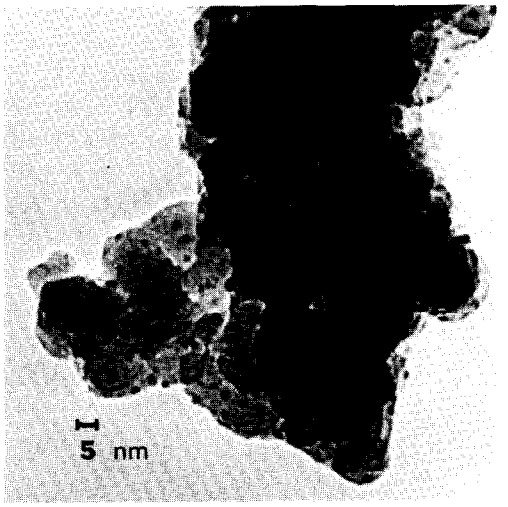

b BEFORE

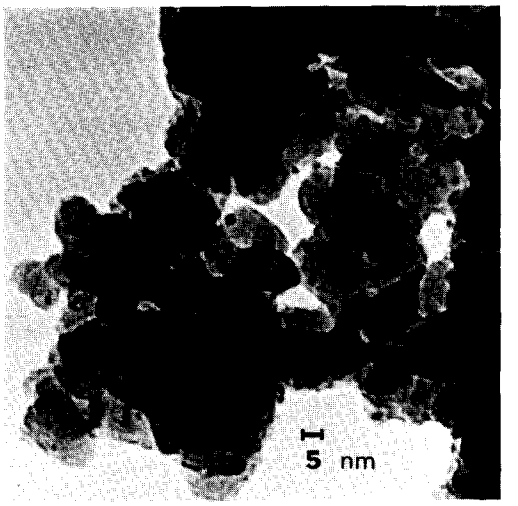

AFTER

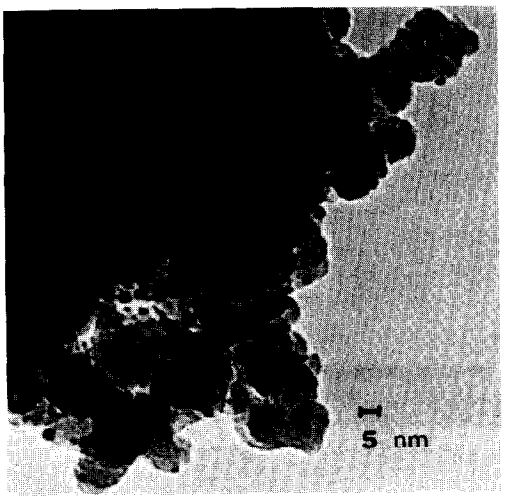

c BEFORE

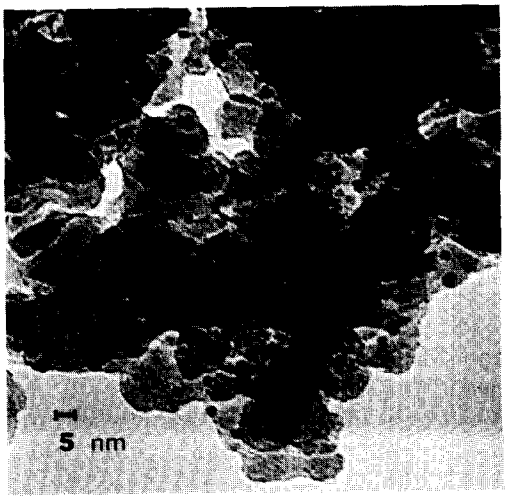

AFTER

TABLE 2

Chemisorption of CO before and after Cycles of CO Adsorption and Desorption

Sample of Pd/SiO_2 Pd particle size (nm)	Percentage of metal exposed before the cycles[a] (%)	Percentage of metal exposed after seven cycles[a] (%)	Particle size determined by BFEM after seven cycles (nm)
1.1	88.4	21.4	<1.0
1.5	79.3	43.7	1.3
2.5	37.9	38.0	2.4

[a] Adsorption at room temperature. Assumed stoichiometry (CO/Pd) = 1.

chemisorption is summarized in Table 2. The loss of CO chemisorption sites were observed to increase as the particle size decreased. However, electron microscopy results of the samples before (Table 1) and after (Table 2) the cycles have indicated that the palladium particles were stable under CO with all three samples. The electron micrographs in Figs. 2a, b, and c show that the large loss of CO chemisorption sites cannot be explained, for example, by the decrease in metal surface area due to extensive sintering of the metal particles. The particle size distributions after the cycles showed narrow peaks for 1.36% Pd/SiO_2 and 1.88% Pd/SiO_2-A and a relatively broad one for 1.88% Pd/SiO_2-B. For the first two samples, almost all of the palladium particles were below 2.0 nm, whereas the majority of the particles were larger than this size for the third sample. The smallest particle observed was 0.8 nm. It should be noted that electron microscopy can be reliable for size determination when chemisorption methods are ambiguous and the term "percentage metal exposed" is more appropriate than the more popular word "dispersion," since the former is not linked to the idea of a particle size while the latter is. Both are equivalent only in the case of uncontaminated surfaces.

With silica alone, CO adsorption and desorption cycles as well as adsorption isotherm measurements at RT were performed. The support had been treated exactly in the same way as the preparation for support with metal deposited on it. Irreversibly adsorbed CO was undetectable, whereas reversibly adsorbed CO was pressure-dependent and the uptake increased linearly with pressure. After adsorption of CO at 50 kPa and evacuation, there was no gas desorption on heating from RT to 673 K. In another experiment, the support was kept under 4.53 kPa of gas phase CO at RT. But the values of A_{des} and A_{read} were equal and both stayed constant. These data indicated that CO adsorbs and desorbs molecularly on the support.

With palladium particles, 1.1 and 1.5 nm in size, gas-phase analysis by a GC/mass spectrometer (Hewlett–Packard 5999A) after three cycles showed an appreciable amount of CO_2 in both cases, and the amount per surface palladium atom increased as the particle size decreased (Table 3). We can see that the specific amounts of CO_2 formed are quantitatively consistent with the results shown in Figs. 1a and b. Trace amounts of dioxygen present as impurity in the original CO could yield only 10^{-3} μmol of CO_2 at the most. Also, surface carbon was detected gas chromatographically by reacting it with dihydrogen, and the amount of methane formed was reasonably equivalent to the amount of CO_2 formed for 1.88% Pd/SiO_2-A. This should be the case if we have CO disproportionation ($2CO = C + CO_2$).

The effect of the gas-phase CO pressure on cycling was also studied. The features in Fig. 1 and Table 2 were the same when CO

FIG. 2. Bright-field electron micrographs of samples before and after cycles of CO adsorption and desorption. (a) 1.36% Pd/SiO_2, (b) 1.88% Pd/SiO_2-A, (c) 1.88% Pd/SiO_2-B.

TABLE 3

Gas-Phase and Surface Analyses after Three Desorption–Readsorption Cycles

Sample of Pd/SiO_2 Pd particle size (nm)	Total amount of surface Pd[a] (μmol)	Total amount of CO_2 detected (μmol)	Total amount of CH_4 detected (μmol)
1.1	52.7	12.4 24% of total surface Pd	Methane detected but not measured quantitatively
1.5	28.3	3.7 13% of total surface Pd	3.0 ± 1.0

[a] From dihydrogen chemisorption at room temperature.

was adsorbed at 50 kPa, but the sample was kept in 4.20 kPa of CO instead of being evacuated prior to the first desorption. However, the declines in A_{des} and A_{read} were steeper. On the other hand, when the system was kept open to the pumping system during each desorption, the changes in these values were similar to those seen in Fig. 1. Thus, the presence of gas-phase CO does enhance the disproportionation, as expected, but it is not an essential requirement for carbon deposition since it is the chemisorbed CO which deposits carbon. This is probably the reason for the consistency between the low-pressure results (*23*) and the present high-pressure results where the same phenomenon of CO disproportionation on small palladium particles was observed.

Infrared Spectroscopy

A series of FT–ir spectra for CO chemisorbed at RT on 1.1-nm particles is shown in Fig. 3. All spectra were obtained after adsorption of CO at 6.67 kPa and evacuation for $\frac{1}{2}$ h at 10^{-5} Pa at RT. After heating to 673 K under 7.76 kPa of CO and evacuation at this temperature, spectrum (b) was obtained. Then the sample was heated to 673 K under vacuum, dihydrogen was flowed for $\frac{1}{4}$ h at atmospheric pressure, and the sample was evacuated for 2 h at 673 K. This resulted in spectrum (c). In comparison with spectrum (a), the intensities of all five absorbance peaks (2084, 2069, 2055, 1920, 1859 cm^{-1}) decreased together in spectrum (b) and increased back together in spectrum (c) for which the peak at 2084 cm^{-1} was fully recovered. These results indicate the loss of CO chemisorption sites

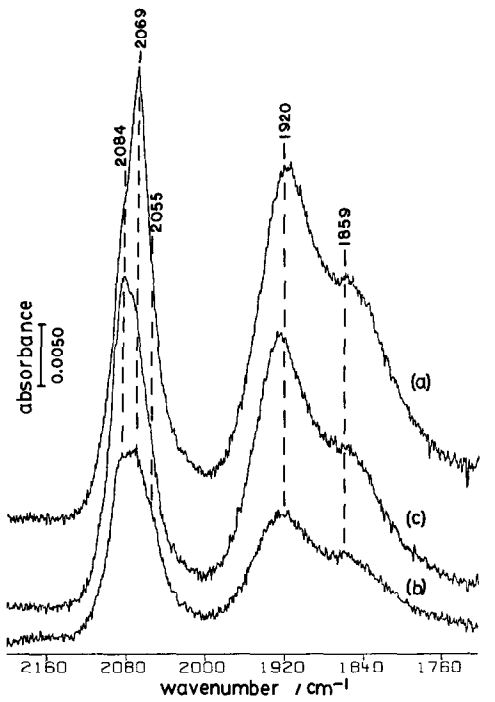

FIG. 3. FT–ir spectra at RT for CO chemisorbed at RT on 1.1 nm Pd/SiO_2. (a) After reduction and evacuation at 673 K. (b) After heating to 673 K under 7.76 kPa of CO and evacuating at 673 K. (c) After dihydrogen treatment and evacuation at 673 K.

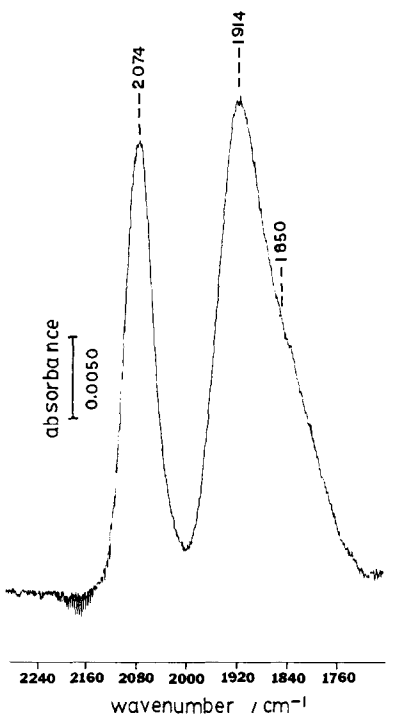

FIG. 4. FT–ir spectrum for CO chemisorbed at RT on 1.5 nm Pd/SiO_2.

after heating with chemisorbed CO and regeneration of the sites by dihydrogen treatment. These observations are consistent with the results of temperature-programmed desorption of CO on palladium particles smaller than 2 nm (*23*). However, there was no large preferential decrease of any specific peak identified in spectrum (b) which would have implied carbon deposition on the particular sites represented by that peak. When the above spectra were taken under 1.33 kPa of CO after adsorption at 6.67 kPa, the peaks appeared at 2169, 2099, 2055, 1941, and 1880 cm^{-1}, the first peak corresponding to physisorbed CO on the support. The peak at 2099 cm^{-1} had an intensity 4.3 times larger than the 1941-cm^{-1} peak. But the trends observed were the same as in Fig. 3 for the variations of the peak intensities although 2169 cm^{-1} remained the same. Also, there were no appreciable shifts in the peak positions when all three spectra were compared. When the gas-phase CO pressure was further increased to 6.72 kPa, the only new feature was the threefold increase in the intensity of the 2099-cm^{-1} peak compared to the spectrum taken under 1.33 kPa of CO. All of the ir spectra have shown that whether in vacuum (10^{-5} Pa) or under some CO pressure, the positions of the absorbance peaks are more or less the same, and they do not shift appreciably under the different pressure conditions. This indicates that the adsorbed states of chemisorbed CO are not very much influenced by the gas-phase CO. The above experiment was also performed in the temperature range near 200 K and RT. But there was no decrease in any of the peaks (2090, 2082, 2051, 1936, or 1853 cm^{-1}) for CO chemisorbed at 200 K after warming to RT in 7.82 kPa of CO. This indicates that carbon deposition does not occur below RT, and the CO chemisorption sites are not lost.

The effect of particle size on the chemisorbed states of CO was observed. Figure 4 shows a spectrum for CO chemisorbed at RT on 1.5-nm particles. This spectrum can be compared with spectrum (a) in Fig. 3. The major absorbance peak above 2000 cm^{-1} increased relative to the major peak below this wavenumber when the particle size decreased. Thus, the relative concentrations of the CO chemisorption sites corresponding to the two major peaks are particle-size-dependent. Similar observation was made on the samples of silica-supported palladium (*24*). In this case under 1 hPa of CO at RT, the ir band intensity for the major peak at relatively high wavenumber increased compared to that at relatively low wavenumber when the palladium particle size decreased from 10.5 to 1.5 nm. According to the electron donation–backdonation scheme first applied to the CO adsorbed on metals by Blyholder (*25*) for the interpretation of ir bands, the population of the relatively weak chemisorbed CO compared to the relatively strongly chemisorbed CO increased as the Pd particles became smaller in our case. Again, we stress

TABLE 4

Reaction between CO and H_2 at 548 K, $H_2/CO = 3$ and Atmospheric Pressure

Pd/SiO_2 catalyst	Percentage of metal exposed	STY_{CH_4}[b] (10^{-4} s^{-1})	Reference
1.36	100	14.7	This work
1.88-A	75.4	14.5	This work
1.88-B	45.4	5.0	This work
4.75	46	3.2	(*14*)
1.93	20	1.2	(*29*)

[a] Selectivity was 100% to methane in all cases.

[b] Site Time Yield (STY_{CH_4}) is defined as the number of CH_4 molecules produced per site per second.

the consistency of this interpretation with that obtained at low pressure (*23*).

New evidence was recently found which specifies the active sites for carbon deposition by CO on ruthenium. Yamasaki *et al.* (*26*) took a series of ir spectra for CO adsorbed at 6.8 kPa on Ru/SiO_2. Their results show that carbon deposition by disproportionation occurred readily on sites for weakly held CO rather than on the sites for strongly held CO. The band intensities for twin-bonded CO (2146 and 2085 cm^{-1}) decreased remarkably at first, then the intensity for linearly bonded CO (2050 cm^{-1}) also decreased slightly after the disproportionation reaction at 423–573 K. Moreover, the twin bands reappeared after hydrogenating the surface carbon into mainly methane. A similar result was obtained recently with a ruthenium cluster (*27*). Dodecacarbonyltriangulo-triruthenium was thermally decomposed at 423 K to form the hexaruthenium carbido-cluster and evolution of CO_2 was observed. Also, carbon deposition was found on small particles of rhodium having 66% metal exposed where sites for weakly bound CO are expected to exist (*6*) since the gem-dicarbonyl species (2100 and 2040 cm^{-1}) was found only for metal particle size below 1 nm and those bigger than 2 nm led to linear and multicentered species on supported rhodium (*28*). Although we did not detect ir bands indicative of multiple carbonyl groups, we may have a similar situation on the small palladium particles where disproportionation occurs on the sites for relatively weakly bonded CO.

Reaction between Carbon Monoxide and Dihydrogen

The catalysts used were the Pd/SiO_2 samples described in Table 1. The steady-state reaction was first studied at atmospheric pressure (Table 4). Under the conditions of this work, selectivity was 100% to methane with all three catalysts. The site time yield for methanation, STY_{CH_4}, is defined as the number of CH_4 molecules produced per second per site where the total number of sites is measured by dihydrogen chemisorption at RT before use, assuming H/Pd = 1. The values of STY_{CH_4} increased almost threefold as the particle size decreased. When methanol vapor was flowed in helium, no methane was detected. Also no increase in STY_{CH_4} occurred by adding methanol to the feed stream. Therefore, methane did not come from methanol. Vannice *et al.* (*14, 29*) found 100% selectivity to methane on Pd/SiO_2 catalysts at the same temperature and pressure, and their results are included in Table 4. The values of percentage metal exposed were determined by the same method as ours for the freshly made samples. The increase in STY_{CH_4} as the particle size decreases is also evident in their results and fits remarkably well into the overall correlation between the activity and the particle size. Thus, the methanation reaction on palladium is structure-sensitive.

In the case of the ruthenium sample mentioned above (*26*), the sites where CO could relatively weakly adsorb were the active sites for disproportionation and also for methanation, and the number of these sites occupied very small portions of the total surface. Such an observation was also made by King (*30*) on Ru/SiO_2 and Ru/Al_2O_3. The surface carbon coming from CO is known to be very reactive. The carbon reacted with dihydrogen to form methane at

TABLE 5

Reaction between CO and H_2 at 673 K, $H_2/CO = 6$ and 535 kPa

Pd/SiO_2 catalyst Pd particle size (nm)	STY_{CH_4} (s^{-1})	STY_{CH_3OH} (s^{-1})	Selectivity
1.1	[a]	Methanol not detected	100% to methane
1.5	[a]	Methanol not detected	100% to methane
2.5	6.36×10^{-3}	1.03×10^{-3}	0.17

[a] Methane formed but not measured quantitatively.
[b] Equal to STY_{CH_3OH}/STY_{CH_4}.

RT on palladium (*23*), ruthenium (*31*), and rhodium (*6*). A larger supply of the active carbon on smaller palladium particles could be the reason for the higher value of STY_{CH_4} for methane formation. Our results indicate that carbon deposition is not necessarily induced by the presence of surface hydrogen as has been suggested for methanation on palladium (*32*). Therefore, the mechanism of methanation is probably the initial carbon deposition by CO followed by successive hydrogenation of the carbon.

Since the equilibrium conversion of CO to methanol under the conditions of Table 4 is low, the reaction was further studied at higher pressures. The results at 535 kPa are shown in Table 5. The catalysts having smaller palladium particle sizes still showed 100% selectivity to methane, but the catalyst with larger particles gave 17% selectivity to methanol. Blank tests with silica demonstrated no activities for either methanation or methanol formation. Thus, the activity and selectivity for the reaction between CO and H_2 depend on the particle size of palladium.

If we review the published work on palladium from the standpoint of particle size effect, we find data consistent with the trends reported in Tables 4 and 5. For example, on Pd/η-Al_2O_3 having 100% metal exposed, methanol was not detected even at 2 MPa and only methane was observed (*18*). However, almost 100% selectivity to methanol was observed under similar pressure condition on Pd/SiO_2 and Pd/γ-AlO_3 having 26 and 27% metal exposed, respectively, and the methanol formation rates were almost the same with both catalysts (*15*). These results can be explained simply by the shift in selectivity due to particle size. Although other factors cannot be ruled out, the effect of particle size is one factor which should not be ignored in the interpretation of the results for CO–H_2 reactions on palladium.

CONCLUSION

Small palladium particles disproportionate CO to surface carbon and CO_2 whereas large particles do not under identical conditions. As a result, methanation occurs on small particles via hydrogenation of carbon deposited by CO. On large particles, CO remains molecular so that methanol can be formed on hydrogenation at pressures high enough to shift the equilibrium in favor of methanol formation. While the selectivity of CO–H_2 reactions on palladium to methanol or methane may also depend on other factors, it is suggested here that particle size alone can be an important factor in controlling this selectivity.[2]

ACKNOWLEDGMENTS

This work was supported by NASA/Ames Grant NCA2-OR745-105 and National Science Foundation Grant NSF-CPE-8219066. Some of this material was presented at an ACS Symposium in June 1983 in San Francisco, and a partial account appeared in American Chemical Society Symposium Series, No. 248, Chap. 23, T. E. Whyte, Jr., R. A. Dalla Betta, E. G. Derovane, and R. T. K. Baker, Editors, American Chemical Society, March 1984.

[2] The difference in selectivity with particle size was observed at lower temperatures as suggested by one of the referees. Before the high-pressure system was built, we worked with a Pyrex system. At 498 K, $H_2/CO = 11$ and 202 kPa, methanol was detected with 1.88% Pd/SiO_2-B catalyst giving $STY_{CH_3OH} = 1.25 \times 10^{-5}$ and $STY_{CH_4} = 4.25 \times 10^{-4}$ s^{-1}. Therefore the selectivity for methanol was 3%. However, the other two catalysts (1.36% Pd/SiO_2 and 1.88% Pd/SiO_2-A) produced only methane, and no methanol was detected at these conditions.

REFERENCES

1. Ford, R. R., "Advances in Catalysis," Vol. 21, p. 51. Academic Press, New York, 1970.
2. Biloen, P., and Sachtler, W. M. H., "Advances in Catalysis," Vol. 30, p. 165. Academic Press, New York, 1981.
3. Brodén, G., Rhodin, T. N., Brucker, C., Benbou, R., and Hurych, Z., *Surf. Sci.* **59,** 593 (1976).
4. Joyner, R. W., and Roberts, M. W., *J. Chem. Soc., Faraday Trans. I* **70,** 1819 (1974).
5. Low, G. G., and Bell, A. T., *J. Catal.* **57,** 397 (1979).
6. Solymosi, F., and Erdohelhi, A., *Surf. Sci.* **110,** 6630 (1981).
7. Doering, D. L., Poppa, H., and Dickinson, J. T., *J. Vac. Sci. Technol.* **17,** 198 (1980).
8. Doering, D. L., Poppa, H., and Dickinson, J. T., *J. Catal.* **73,** 91 (1982).
9. Araki, M., and Ponec, V., *J. Catal.* **44,** 439 (1976).
10. Rabo, J. A., Risch, A. P., and Poutsma, M. L., *J. Catal.* **53,** 295 (1978).
11. Biloen, P., Helle, J. N., and Sachtler, W. M. H., *J. Catal.* **58,** 95 (1979).
12. Sachtler, J. W. A., Kool, J. M., and Ponec, V., *J. Catal.* **56,** 284 (1979).
13. Solymosi, F., Tombácz, I., and Kocsis, M., *J. Catal.* **75,** 78 (1982).
14. Vannice, M. A., *J. Catal.* **40,** 129 (1975).
15. Poutsma, M. L., Elek, L. F., Ibaria, P. A., Risch, A. P., and Rabo, J. A., *J. Catal.* **52,** 157 (1978).
16. Fajula, F., Anthony, R. G., and Lunsford, J. H., *J. Catal.* **73,** 237 (1982).
17. Ryndin, Yu, A., Hicks, R. F., and Bell, A. T., *J. Catal.* **70,** 287 (1981).
18. Vannice, M. A., and Garten, R. L., *Ind. Eng. Chem. Prod. Res. Dev.* **18,** 186 (1979).
19. Kikuzono, Y., Kagami, S., Naito, S., Onishi, T., and Tamaru, K., *Faraday Discuss. Chem. Soc.* **72,** 135 (1981).
20. Poels, E. K., Koolstra, R., Geus, J. W., and Ponec, V., *in* "Metal-Support and Metal-Additive Effects in Catalysis" (B. Imelik *et al.*, Eds.), p. 233. Elsevier, Amsterdam, 1982.
21. Hwang, H. S., Ph.D. dissertation, Stanford University, 1975.
22. Ladas, S., Dalla Betta, R. A., and Boudart, M., *J. Catal.* **53,** 356 (1978).
23. Ichikawa, S., Poppa, H., and Boudart, M., "ACS Advances in Chemistry Series" (T. E. Whyte, R. A. Dalla Betta, E. G. Derovane, and R. T. K. Baker, Eds.), No. 248, Chap. 23, pp. 439–452. Amer. Chem. Soc., Washington, D.C., 1984.
24. van Hardeveld, R., and Hartog, F., "Advances in Catalysis," Vol. 22, p. 75. Academic Press, New York, 1972.
25. Blyholder, G., *J. Phys. Chem.* **68,** 2772 (1964).
26. Yamasaki, H., Kobori, Y., Naito, S., Onishi, T., and Tamaru, K., *J. Chem. Soc. Faraday Trans. I* **77,** 2913 (1981).
27. Nicholls, J. N., Farrar, D. H., Jackson, P. F., Johnson, B. F. G., and Lewis, J., *J. Chem. Soc.* **8,** 1395 (1982).
28. Kaufherr, N., Primet, M., Dufaux, M., and Naccache, C., *C.R. Ser. C.* **286,** 131 (1978).
29. Vannice, M. A., Wang, S-Y., and Moon, S. H., *J. Catal.* **71,** 152 (1981).
30. King, D., "Symposium on Advances in Fischer–Tropsch Chemistry." Amer. Chem. Soc., Anaheim Meeting, 1977.
31. Low, G. G., and Bell, A. T., *J. Catal.* **57,** 397 (1979).
32. Wang, S-Y., Moon, S. H., and Vannice, M. A., *J. Catal.* **71,** 167 (1981).